Effects of Intermediate Filter Thickness on the Detective Quantum Efficiency of Sandwich Detectors for Dual-Energy X-ray Imaging

Junwoo Kim [a], Dong Woon Kim[a], Soohwa Kam[a], Hanbean Youn [a], Ho Kyung Kim [a,b*]
[a]*School of Mechanical Engineering, Pusan National University, Busan, South Korea*
[b]*Center for Advanced Medical Engineering Research, Pusan National University, Busan, South Korea*
[*]*Corresponding author: hokyung@pusan.ac.kr*

1. Introduction

The double-shot dual-energy imaging (DEI) can discriminate, or enhance, material content (e.g., bone or soft tissue) within a two-dimensional radiograph and can provide improved visualization of lesions for clinician [1]. Existing double-shot DEI system uses the fast kilovoltage (kV) switching technique (also known as the double-shot or double-exposure technique). However, the double-shot technique is susceptible to motion artifacts resulting from an anatomical mismatch between two successive exposures [2].

Single-shot DEI using a sandwich detector that is configured by stacking two detectors can provide motion-artifact-free dual-energy images, because the sandwich detector obtain low and high energy images at a single exposure. In our previous study [3], we introduced the flat-panel sandwich detector and successfully demonstrated by providing bone and soft tissue-enhanced mouse images. For the practical use of the sandwich detector in preclinic or clinic, however, optimization studies on the design and techniques are further required.

In this study, we quantitatively evaluate the imaging characteristics, such as modulation transfer function (MTF), noise power spectrum (NPS), and detective quantum efficiency (DQE) of each front and rear detector layer. Especially, we focus on the effect of the intermediate copper (Cu) filter thickness on the imaging characteristic.

2. Materials and Methods

2.1 Sandwich Detector System

The sandwich detector used in this study is built by stacking two flat-panel detectors (FPDs), each of which employs a different phosphor (thinner for the front and thicker for the rear layer). Figure 1 illustrates the operation principle of single-shot DEI using the sandwich detector. Each FPD consists of a phosphor, which converts the x-ray photons to optical photons, and a photodiode array, which detect the optical photons and converts to electric signal. For the phosphor layers, we use commercial phosphor screens based on terbium-doped gadolinium oxysulfide (Gd_2O_2S:Tb). The front FPD employs a thinner phosphor (Min-R^{TM} 2000, Carestream Health Care Inc., USA) and phosphor thickness is 0.085 mm, and we call simply the high resolution phosphor (HR). Considering the attenuation of

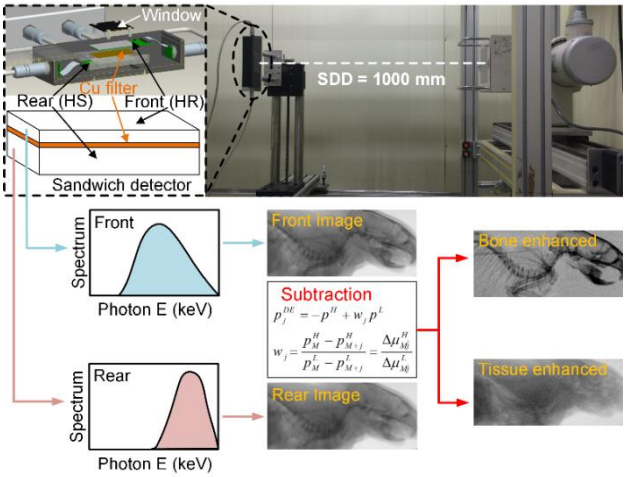

Fig. 1. Computer-aided design drawing for housing and schematic illustration of the operation principle of single-shot DEI that obtained for a postmortem mouse.

x-ray photons after passing through the front FPD, we use a thicker phosphor (Lanex^{TM} Regular) with a thickness of 0.18 mm at the rear FPD, and we call the high sensitivity phosphor (HS) [4].

The photodiode array (RadEye1^{TM}, Teledyne DALSA Inc., Sunnyvale, CA) is fabricated by the complementary metal-oxide-semiconductor (CMOS) process, and it features 0.048 mm-sized pixels arranged in 1024×512 format. Therefore, the active imaging area was about 50 $\times$ 25 mm^2. We place a thin Cu filter between two FPDs to enhance x-ray beam hardening. The sandwich detector is enclosed in a light-tight box made of aluminum (Al), which opens a 1 mm-thick polycarbonate window for x-ray irradiation.

2.2 Experimental Setup

For single-shot DEI conditions, we use 60 kVp tungsten spectra (E7239X, Toshiba Inc.) without additional filtration. The source-to-detector distance is fixed at 1000 mm. Detector integration time is 0.2 seconds.

2.2 Fourier Metrics

The MTF is the contrast transfer function in terms of spatial frequency. The MTF can be calculated by the fourier transformation of the fine-sampled line-spread functions which is resulted from the differentiation of the profiles extracted from the edge images (i.e. edge spread

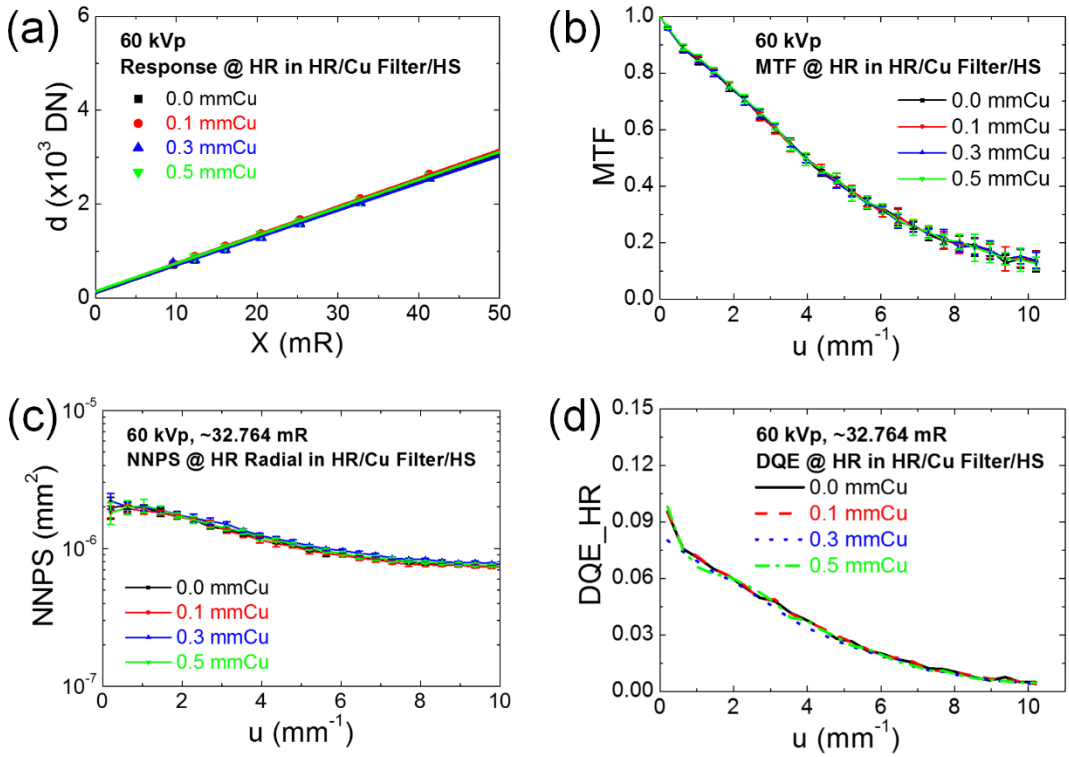

Fig. 2. Imaging charateristics of the "Front" detector in the sandwich configuration: (a) Response, (b) MTF, (c) NNPS, (d) DQE

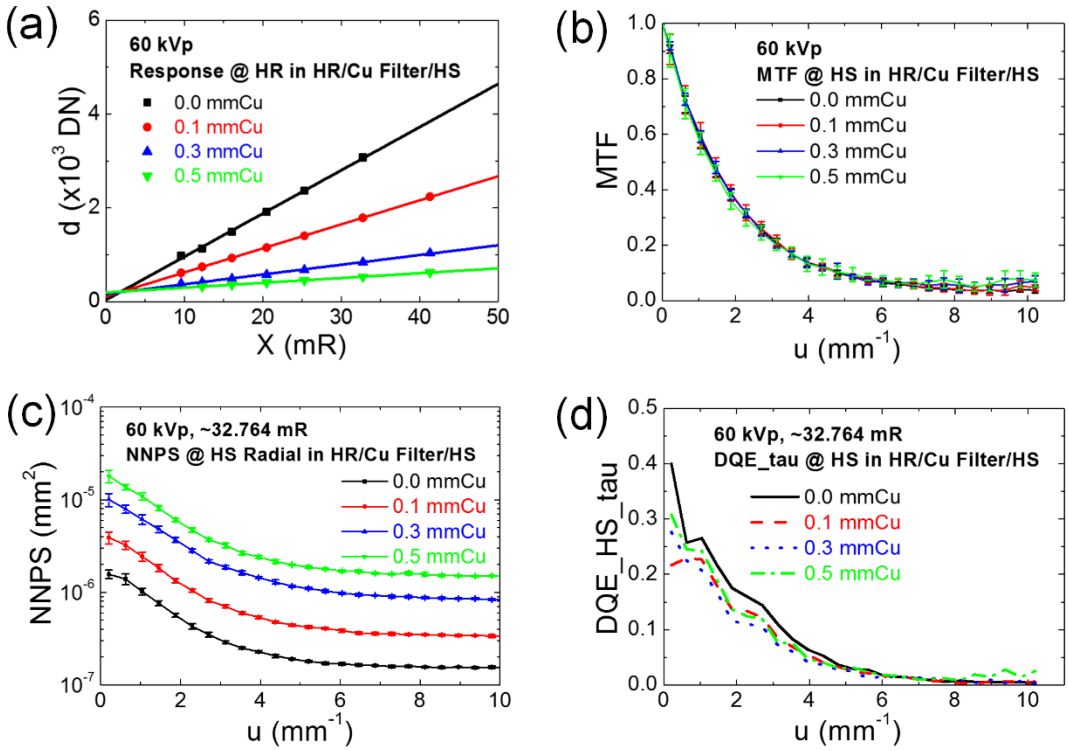

Fig. 3. Imaging charateristics of the "Rear" detector in the sandwich configuration: (a) Response, (b) MTF, (c) NNPS, (d) DQE

functions, ESFs) [5, 6]. Therefore, we can have

$$\mathrm{MTF}_j(u) = \mathrm{FT}\left\{\frac{\partial \mathrm{ESF}(x)}{\partial x}\right\}, \quad (1)$$

where the subscript j denotes the detector layer.

The NPS is a spectral decomposition of the variance [7]. We normalize the NPS by the mean pixel value of white images, hence NNPS:

$$\mathrm{NNPS}_j(u) = \frac{1}{\mathrm{A}_{ROI}} \left\langle \left[FT\left\{ \frac{d(u) - \overline{d(u)}}{\overline{d(u)}} \right\} \right]^2 \right\rangle, \quad (2)$$

where A_{ROI} denotes the number of image ROI.

In this study, the j th detector DQE is given by [4, 8]

$$\mathrm{DQE}_j(u) = \frac{\mathrm{MTF}_j^2(u)}{\mathrm{NNPS}_j(u) \times \overline{q_0} \times \tau_j}, \quad (3)$$

where $\overline{q_0}$ is the incident x-ray photon fluence at the surface of the front detector and τ_j denotes the transmittance of $\overline{q_0}$ through the front detector and the Cu filter. Therefore, we note that $\tau_F = 1$.

3. Results

Figure 2 shows the imaging characteristics of the front HR detector. Figure 2(a) shows the characteristic curves that are the mean pixel values as a function of exposure. Figures 2(b), (c), and (d) represent the MTF, NNPS, and DQE of the front HR detector with respect to various Cu thicknesses. All the imaging characteristics are independent of the Cu thicknesses used as the intermediate filter.

Figure 3 shows the imaging characteristics of the rear HS detector. Unlike the front detector, the response of the rear detector is decreased with increasing Cu thickness, as shown in Fig. 3(a), and this observation can be readily expected because of decreasing photon fluence with increasing Cu thickness. As shown Fig. 3(b), we find that the MTF is almost independent of the Cu thickness. On the other hand, the NNPS degrades as the Cu thickness increases, as shown in Fig. 3(c). This observation can be explained by the increased additional noise that is relatively higher than the quantum noise. We believe that the additional noise is the electronic noise which is not negligible when the $\overline{d}$ becomes low. However, the decreasing $\overline{d}$ and increasing NNPS with increasing Cu thickness provide the almost same DQE performance, as shown in Fig. 3(d).

4. Conclusions and Further Study

We have built the sandwich detector for the single-shot DEI. In order to quantitatively evaluate the imaging performance, we measured the characteristic curve, MTF, NNPS, and DQE of the sandwich detector. The imaging characteristics of the front detector are barely affected by the sandwich structure. On the other hand, a thicker filtration reduces the rear detector response and degrades the NNPS. The MTF of the rear detector is not affected by variations in the Cu filter. Therefore, we obtain the DQE that is almost independent of the Cu filter thicknesses. We will investigate the DQE for various combinations of phosphor thicknesses and incident x-ray spectra.

ACKNOWLEDGEMENT

This work was supported by the National Research Foundation of Korea (NRF) grants funded by the Korea governments (MSIP) (No. 2013M2A2A904613 and No. 2014R1A2A2A01004416).

REFERENCES

[1] N. A. Shkumat, J. H. Siewerdsen, A. C. Dhanantwari, D. B. Williams, S. Richard, N. S. Paul, J. Yorkston, and R. Van Metter, Optimization of imaging acquisition techniques for dual-energy imaging of the chest, *Med. Phys.*, Vol. 34, No. 10, pp. 3904-3915, 2007.

[2] G. J. Gang, C. A. Varon, H. Kashani, S. Richard, N. S. Paul, R. Van Metter, J. Yorkston, and J. H. Siewerdsen, Multiscale deformable registration n for dual-energy x-ray imaging, *Med. Phys.*, Vol. 36, No. 2, pp. 351-363, 2009.

[3] J. C. Han, D. W. Kim, S. Yun, H. Youn, S. Kam, and H. K. Kim, Dual-energy imaging with an active sandwich detector, presented at the *2013 IEEE* Nuclear Science and Medical Imaging Conference, and Workshop on Room-Temperature Semiconductor X-ray and Gamma-ray Detectors, Seoul, Korea, Oct. 27–Nov. 2, 2013.

[4] M. K. Cho, H. K. Kim, T. Graeve, S. M. Yun, C. H. Lim, H. Cho, and J.-M. Kim, Measurements of x-ray imaging performance of granular phosphors with direct-coupled CMOS sensors, *IEEE Trans. Nucl. Sci.*, Vol. 55, No. 3, pp. 1338-1343, 2008.

[5] H. Fujita, D. Y. Tsai, T. Itoh, K. Doi, J. Morishita, K. Ueda, and A. Ohtsuka, A simple method for determining the modulation transfer function. *IEEE Trans. Med. Imaging*, Vol. 11, No. 1, pp. 34-39, 1992.

[6] E. Samei, M. J. Flynn, and D. A. Reimann, A method for measuring the presampled MTF of digital radiographic systems using an edge test device, *Med. Phys.*, Vol. 25, No. 1, pp. 102-113, 1998.

[7] M. B. Williams, P. A. Mangiafico, and P. U. Simoni, Noise power spectra of images from digital mammography detectors. *Med. Phys.*, Vol. 26, No. 7, pp. 1279-1293, 1999.

[8] I. A. Cunningham and R. Shaw, Signal-to-noise optimization of medical imaging systems, *J. Opt. Soc. Am. A*, Vol. 16, pp. 621-632, 1999.